

Original Research

Antibody-Based Capture and Behaviour of Endothelial Cell Lines on Pre-Surface Modified Medical Grade Steel

Rohan R. Ravindranath ¹, Brian De La Franier ¹, Issaka Yougbare ², Jason E. Fish ³, Michael Thompson ^{1,*}

1. Department of Chemistry, University of Toronto, 80 St. George Street, Toronto, Ontario M5S 3H6, Canada; E-Mails: ravindranath.rohanr@gmail.com; brian.delafanier@mail.utoronto.ca; m.thompson@utoronto.ca
2. Toronto Platelet Immunobiology Group and Department of Laboratory Medicine, Keenan Research Centre for Biomedical Science, St Michael's Hospital, Toronto, Ontario M5B 1W8, Canada; E-Mail: issaka.yougbare@sanofipasteur.com
3. Toronto General Hospital Research Institute, University Health Network, Toronto, Ontario M5G 1L7, Canada; E-Mail: jason.fish@utoronto.ca

* **Correspondence:** Michael Thompson; E-Mail: m.thompson@utoronto.ca

Academic Editor: Hossein Hosseinkhani

Special Issue: [Applications and Development of Biomaterials in Medicine](#)

Recent Progress in Materials
2020, volume 2, issue 1
doi:10.21926/rpm.2001008

Received: January 25, 2020
Accepted: March 25, 2020
Published: March 27, 2020

Abstract

Coronary artery disease is one of the major causes of morbidity and mortality worldwide. Coronary stents, tube-shaped medical implants that are placed in narrowed coronary arteries, have been used successfully in the management of this condition. However, re-narrowing (i.e. restenosis) of the artery can occur which is instigated by an immune response towards the implanted 'foreign' material. A new approach to prevent restenosis and reduce the stent-induced immune response has been proposed previously, which involves re-endothelialization of the implanted stent. In the present study a proof-of-concept experiment involving surface-modified medical grade steel was employed in order to examine the best surface chemistry for in vitro cell capture. Steel coupons were coated with



© 2020 by the author. This is an open access article distributed under the conditions of the [Creative Commons by Attribution License](#), which permits unrestricted use, distribution, and reproduction in any medium or format, provided the original work is correctly cited.

a silanized adlayer, followed by attachment of whole antibodies, followed by culturing of human umbilical vein endothelial cells (HUVECs) or human aortic endothelial cells (HAECs or HAoECs). With regard to the adlayer-antibody configuration, HUVECs adhered and grew with normal morphology, and a significantly increased number of HUVECs proliferated on the coupons compared to the 'bare' surface. Similar effects were observed with HAECs grown on adlayer-antibody modified substrates, with a significantly higher number of cells proliferating. These results demonstrate a successful strategy for re-endothelialization of the steel surface that may prevent immune response with respect to the behaviour of steel-based stents in vivo.

Keywords

Self-assembled monolayer; endothelial cell; coronary stent; biocompatibility; re-endothelialization

1. Introduction

Coronary artery disease (CAD), which is a leading cause of death, is characterized by plaque build-up along arterial walls [1-3]. This process is known as atherosclerosis, and leads to complications such as loss of arterial elasticity and narrowing of the arteries (stenosis) [1-3]. Atherosclerosis typically affects the intima (inner layer), and can obstruct the flow of blood from occurring smoothly [4, 5]. Within the intima, the endothelial 'layer' possesses antithrombotic properties, such as the ability to release nitric oxide (NO) [4, 5]. Atherosclerotic plaque is composed of a variety of biological materials including lipids and fibrous tissue [6]. If the heart receives insufficient blood flow due to obstruction caused by thrombi, chest pain may develop and this condition is known as angina [7]. A myocardial infarction or heart attack has the potential to develop in this case.

It has been estimated that approximately 40.5% of the American population will possess some form of cardiovascular disease by 2030 [8]. Over the last few decades, coronary bypass surgery, balloon angioplasty, and more recently, development of coronary stents have been proposed to combat stenosis [9]. Stents are implantable tubular structures that are used to open up restricted arteries [10]. In reality, however, it is very common for aggregates of platelets and fibrin to form thrombus on the surface of the coronary stent. Without adequate options to treat the thrombus formation, this can diminish the beneficial effects of the stent implant such that restenosis can occur. Stent thrombosis can often lead to acute myocardial infarction and death. Given the potential occurrence of restenosis numerous approaches have been employed in attempts to ameliorate the problem largely through the imposition of a variety of surface coatings. Example strategies have been surface additions of drugs, polymeric species and endothelial cells. There has also been research on the alteration of stent surfaces based on the so-called nanomedicine approach.

Drug eluting stents (DES) are coated with an anti-proliferative drug molecule such as Paclitaxel or Rapamycin (Sirolimus) [10-12]. These stents gradually release bound drugs in order to prevent proliferation of smooth muscle cells (SMC) in the lining of the artery, thereby preventing

restenosis and blood clotting. The use of DES however does not necessarily improve the risk of developing thrombosis. In fact a concern associated with DES is that patients with these implants are at an increased risk of developing late stent thrombosis (~30 days to 1 year upon implantation of the stent) [13]. A major cause of this is suggested to be due to poor re-endothelialization of the stent and consequently poor healing of the artery [13].

With respect to the “nano” world Kushwaha *et al.* [14] reported the use of a self-assembled nanofibrous matrix composed of a mixture of peptide amphiphiles onto a metal stent surface. Given the antithrombotic properties of NO a polylysine group was intentionally used in their matrix so that it would have nitric oxide (NO) donating residues. This helps mimic a natural endothelial extracellular matrix (ECM). Endothelial cell proliferation was also increased with this nanofibrous matrix suggesting that the coating may in fact be successful in preventing stent thrombosis. In a similar study performed by Andukuri *et al.* [15] the authors demonstrated a significant decrease in the number of platelets that adhered to a hybrid biomimetic nanomatrix composed of electrospun polycaprolactone (e-PCL) nanofibres attached to self-assembled peptide amphiphiles. Karagkiozaki *et al.* [16] suggested the use of carbon nanocoatings on stainless steel and silicon wafers using radio frequency magnetron sputtering deposition. This was based on the premise that surface roughness has an effect on the adsorption of platelets. Platelet activation was said to be decreased on surfaces containing the nanocoating with high surface roughness.

There has also been significant research on the reduction of platelet adhesion originating from the enormous literature on solid surface-blood interaction chemistry (reviewed in reference 17). Two examples of this sort approach are provided by the work of Whelan *et al.* [18] and Thierry *et al.* [19]. In the former study a phosphorylcholine stent coating was employed to assess the biocompatibility in a porcine model for use in a drug-eluting stent. Coated and uncoated stents were implanted into the coronary arteries of pigs, and were assessed before and after implantation. In the second study two polysaccharides, hyaluronan (HA) and chitosan (CH), were used to form a self-assembled stent coating on a NiTi substrate in a layer-by-layer fashion. Interestingly there was a 38% decrease in platelet adhesion with the NiTi surfaces coated with HA/CH compared to unmodified NiTi.

Finally, re-endothelialization of both injured, natural vascular tissue, and implanted stents for the prevention of platelet aggregation has attracted considerable attention over the years [20-29]. With specific regard to the latter biologically-active surface coatings with the capacity to capture circulating endothelial cells have been proposed. A polyethylene glycol (PEG) adlayer was applied on stainless steel stents as reported by Lee *et al.* [26]. The goal was to immobilize VE-cadherin antibodies on the stent surface in order to capture circulating EPCs and human umbilical vein endothelial cells (HUVECs). *In vitro*, stainless steel stents coated with VE-cadherin antibody were more selective and specific towards EPCs and human umbilical vein endothelial cells (HUVECs) compared to stents coated with CD34 antibody. *In vivo*, stents coated with anti-VE-cadherin promoted re-endothelialization and reduced neointimal hyperplasia (42 days after implantation) compared to the CD34 antibody coated stent counterpart. In another investigation, Li *et al.* [27] explored the efficacy of using anti-CD133 in capturing EPCs by incubating stents immobilized with anti-CD133 antibody in CD133+ cells for 14 days. CD133 is a stem cell marker for hematopoietic stem/progenitor cell (HSPCs). The authors were able to show that stents coated with anti-CD133 resulted in improved EPC capture and attachment, compared to stents modified with a copolymer of L-lactide (LLA) and 5-methyl-5-benzoyloxycarbonate-1,3-dioxan-2-one (MBC) alone.

The Genous endothelial progenitor cell (EPC) capturing stent produced by Orbus Neich Medical Technologies, Fort Lauderdale, FL, USA) has been examined by several groups. For example, in an earlier study it was shown in an AV shunt construction in human CAD patients and baboons that the CD34+ EPC recruitment via the Genous device promotes re-endothelialization and inhibited platelet adhesion. The authors were encouraged by the promising results [28]. In an interesting Korean study the efficacy of the Genous stent was compared with conventional DES stents in a number of patients [29]. The result was that the complete re-endothelialization achieved with the EPC stent “may” provide clinical benefits over DESs, especially in patients with microvascular dysfunction – not exactly rousing support of EPC stent technology.

In previous work, we proposed the use of a bifunctional trichlorosilane linker, benzenethiosulfonate (BTS), which, importantly, has the potential to form a *covalently-attached* surface adlayer for the immobilization of antibodies against cell receptors and, in turn, recruit circulating cells [30]. This surface linker is able to bind to any surface containing surface hydroxyl groups, and therefore can coat a variety of substrates including metals and polymers. We have shown that such a system was able to bind a target antigen specifically, which behaves as a proof-of-concept model for stents [30]. Herein we demonstrate that this biologically active protocol is successful in the capture of endothelial cells and surface re-endothelialization. This was accomplished by testing two different human cell lines in the system, with whole antibodies being employed to capture the cells.

2. Materials and Methods

2.1 Reagents and Solutions

Anhydrous toluene (99.8%), methanol (ACS grade, $\geq 99.8\%$), toluene (ACS grade $\geq 99.5\%$), chloroform (ACS grade, $\geq 99.8\%$) and trichloro(octadecyl)silane ($\geq 90\%$) were purchased from Sigma-Aldrich. Pentane (spectrograde, $\geq 98\%$), acetone (spectrograde, $> 99\%$) and concentrated sulfuric acid (reagent grade, $> 95\%$) were purchased from Caledon Laboratories Ltd. Hydrogen peroxide (ACS grade, 30%) was purchased from Fischer Scientific. Purified anti-human CD144 (VE-cadherin), anti-human CD31 (PECAM-1) and Alexa Fluor® 594 anti-human CD144 antibodies were purchased from Biolegend. Paraformaldehyde (16%) was purchased from Electron Microscopy Sciences. Bovine Serum Albumin was purchased from Wisent. Trypsin-EDTA (0.05%) was purchased from Gibco. All chemicals and reagents were used without further purification.

Phosphate-buffered saline (PBS) was prepared with 154 mM NaCl and 10 mM sodium phosphate dibasic in DI water. The pH was adjusted to 7.2. DI water was deionized water with a resistivity $\geq 18.0 \text{ M}\Omega \cdot \text{cm}$.

Primary human umbilical vein endothelial cells (HUVECs) were regularly procured from Dr. Philip Marsden's lab at St. Michael's Hospital. Telomerase-immortalized human aortic endothelial cells (Telo-HAECs) were obtained from Dr. Jason Fish's lab at Toronto General Research Institute. EGM-2 BulletKit for HUVECs was purchased from Lonza Group. Endothelial Cell Growth Medium MV for HAECs was purchased from PromoCell GmbH. Both cell media were supplemented with 5 mL (per 500 mL) of pen strep (penicillin and streptomycin).

2.2 Cleaning and Surface Modification of Stainless Steel

Austenitic type 316L stainless steel with a mirror polished finish was obtained from Stainless Supply Ltd. in Monroe, North Carolina. The stainless steel was shear cut into 3/8" x 3/8" coupons, with a thickness of .0480". Upon procuring the steel coupons, they were electrochemically polished.

The stainless steel coupons were handled with cleaned stainless steel tweezers on the edges, so that surface contamination and scratches would be avoided. Glassware used for the silanization of stainless steel coupons (20 mL scintillation vials and 150mm test tubes), were pre-treated with trichloro(octadecyl)silane (OTS) in anhydrous toluene (1/20 v/v), overnight. The glassware was treated inside a glove box under inert (N_2) and anhydrous conditions (P_2O_5).

Under these same conditions each steel coupon was fully submerged in a solution of 1:1000 BTS:anhydrous toluene, sealed, and placed on a rotator for 90 minutes under gentle rotation (Figure 1). The samples were then rinsed copiously with toluene, followed by sonication in toluene for 5 minutes. This rinsing and sonication was repeated using 95% ethanol, and then samples were dried under a gently stream of air.

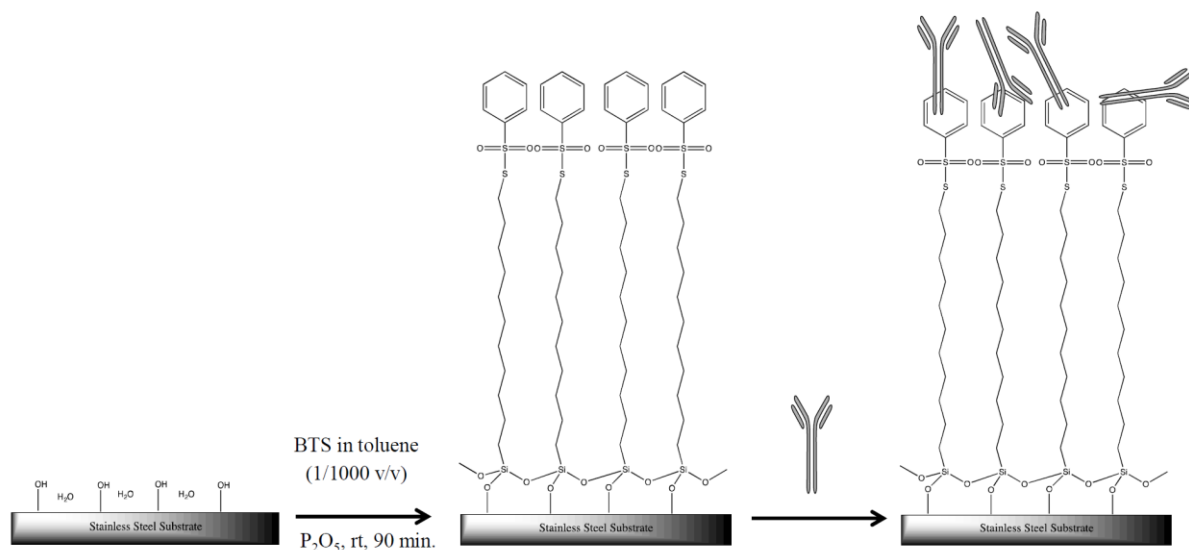


Figure 1 Schematic showing 'bare' stainless steel substrate (left) coated with BTS linker (centre) and antibodies (right).

2.3 Whole Antibody Attachment

Anti-CD144 and anti-CD31 Antibodies were prepared by diluting the commercially available antibody solution (500 $\mu\text{g}/\text{mL}$) to 27.5 $\mu\text{g}/\text{mL}$ with PBS. Anti-CD144 and anti-CD31 were immobilized on the surface of bare and BTS coated steel, by soaking the coupons in the antibody solution. Each sample was placed in a cleaned test tube with the "right-side" facing up, and 650-750 μL of antibody solution was transferred to each test tube. The test tubes were then stoppered with a rubber septum, covered in tin foil and placed on a spin plate for 14-18 h. The following day, the antibody solution from each test tube was removed and each coupon was rinsed with 15 mL of filtered PBS and 15 mL of deionized water. The coupons were then dried under a gentle stream of N_2 and stored at 4°C until they were used for cell culture and perfusion experiments.

2.4 XPS Surface Analysis

Angle-resolved XPS analysis was performed with a Theta Probe Angle-Resolved X-ray Photoelectron Spectrometer System (Thermo Fisher Scientific Inc., Waltham, MA, USA) located at Surface Interface Ontario (University of Toronto, Toronto, ON, Canada) for steel coupons set aside before and after, each step of chemical surface modification, and immobilization of antibodies. The samples were analyzed with monochromated Al K α X-rays (elliptical spots of 400 μ m along the long axis) with take-off angles of 90° relative to the surface. Peak fitting and data analysis were performed using the *Avantage* software provided with the instrument.

2.5 Cell Cultures: HUVECs and HAECs.

Primary cells and cell line cultures were obtained from their respective sources, and passaged into larger T-75 flasks (Corning Life Sciences). Next, confluent cells were washed and 4 mL of trypsin was put into each culture and incubated at 37°C for 4 min. Twice the amount of cell media was added to the culture, to quench the action of trypsin. The solution containing cells was transferred to a 50 mL centrifuge tube and was centrifuged for 5 min at 400 xg. The supernatant was discarded and the cell pellet was re-suspended in 2-3 mL of fresh media. A volume of 1 mL of the re-suspended cells was added to a new T-75 cell culture flask, along with 9 mL of fresh cell media. Cells were monitored and grown until confluence under standard cell culture conditions (37°C, 5% CO₂). Cell media was changed every 48 h. After the cells had reached confluence, they were seeded onto each of the stainless steel samples following the passaging procedure above. Each steel coupon was placed in a 24-well cell culture plate. Upon re-suspension of cells in fresh media, they were counted using a standard hemocytometer to ensure equal distribution of cells per sample. The cells were then equally aliquoted onto each sample, and cell media was added to bring each well to a final volume of 1 mL. The cells were cultured on the steel samples for 3-5 days before they were processed for fluorescence imaging.

2.6 Cell Fixation and Staining with Fluorescently Labeled Primary Antibody

Cells were fixed with 4% PFA (in PBS) for 15 min. The stainless steel coupons were then blocked for 30 min. using 5% BSA, which was diluted in 1X PBS-T. Following BSA treatment each coupon was stained with Alexa Fluor® 594 anti-human CD144. The commercially bought antibodies were diluted in 1% BSA in 1X PBS-T (1/200). Each sample was immersed in 800 μ L of the solution, and placed on the spin plate in the dark for two hours. This was done to avoid photo bleaching of the fluorophore. Two hours later the coupons were rinsed four times with 1 mL of 1X TBS-T. After the fourth rinse they were stored in 1X PBS at 4°C.

2.7 Fluorescence Microscopy

Fluorescence microscopy was completed at the Advanced Optical Microscopy Facility (AOMF), University Health Network (UHN) in Toronto, Ontario. A Zeiss AxioImager Z1 upright fluorescence microscope was used with a Hamamatsu Flash4 camera. 10x/0.3 EC Plan-Neofluar objective lens was used along with Texas red longpass and DAPI filters. Images were acquired using Metamorph, and processed using ImageJ software.

Confocal microscopy was also performed at the Advanced Optical Microscopy Facility (AOMF), University Health Network (UHN) in Toronto, Ontario. A Zeiss LSM700 inverted confocal microscope was used, with solid-state lasers capable of excitation lines from UV to red. This microscope was equipped with an APO-CHROMAT 40x/1.4 Oil lens. The images were acquired using LSM Zen 2012 software, and were processed using ImageJ.

2.8 Statistical Analysis

Data shown are mean \pm SD. Statistical comparisons were made using an unpaired Student's T test. Immunofluorescence analysis was performed using Image J software (National Institutes of Health) and values were normalized to internal control. Differences were considered statistically significant when $p < 0.05$.

3. Results

Employing the surface modification protocol for stainless steel (Figure 1) that was published by our group previously [30], our objective in this study was to assess how effective the surface modification strategy is with respect to the adherence and growth of HUVECs on steel surfaces *in vitro*.

3.1 XPS Surface Analysis

XPS surface analysis was used to determine the elemental composition of bare and BTS modified steel coupons, as well as with antibodies (Figure 2). This analysis showed the bare steel to have a high concentration of both carbon and oxygen on the surface, due to oxidation of the steel as well as contamination. It also showed a moderate concentration of both chromium and iron. Following incubation with the antibody CD144, the bare steel showed only minor changes to the chemical composition, with a slight increase in carbon and nitrogen signals, and slight decrease in oxygen signal. Incubation with antibody CD31 showed virtually no change from the bare steel except for a slight increase in nitrogen. This suggests that the antibodies were poorly able to bind to the surface.

BTS modified steel showed a large increase in carbon, sulfur, and silicon signal versus bare steel, as well as a decrease in oxygen, chromium, and iron signals. This strongly suggests the BTS linker, which is composed predominantly of carbon, silicon, and sulfur, was able to bind to the steel surface due to the increase in these elements' signals. The reduction in iron, oxygen, and chromium signals also suggests a near complete surface coverage, due to masking the elements present in the steel surface.

Once the antibodies were introduced to the BTS modified steel a large increase in nitrogen was observed, as well as a decrease in sulfur and silicon signals. This suggests that the antibodies were able to bind to the surface, as nitrogen is a common element found in antibodies, as well as masking the sulfur and silicon signals of the linker. The increase in nitrogen is also far larger than was observed for antibodies introduced to bare steel surfaces, suggesting the antibodies are much better able to bind BTS coated steel.

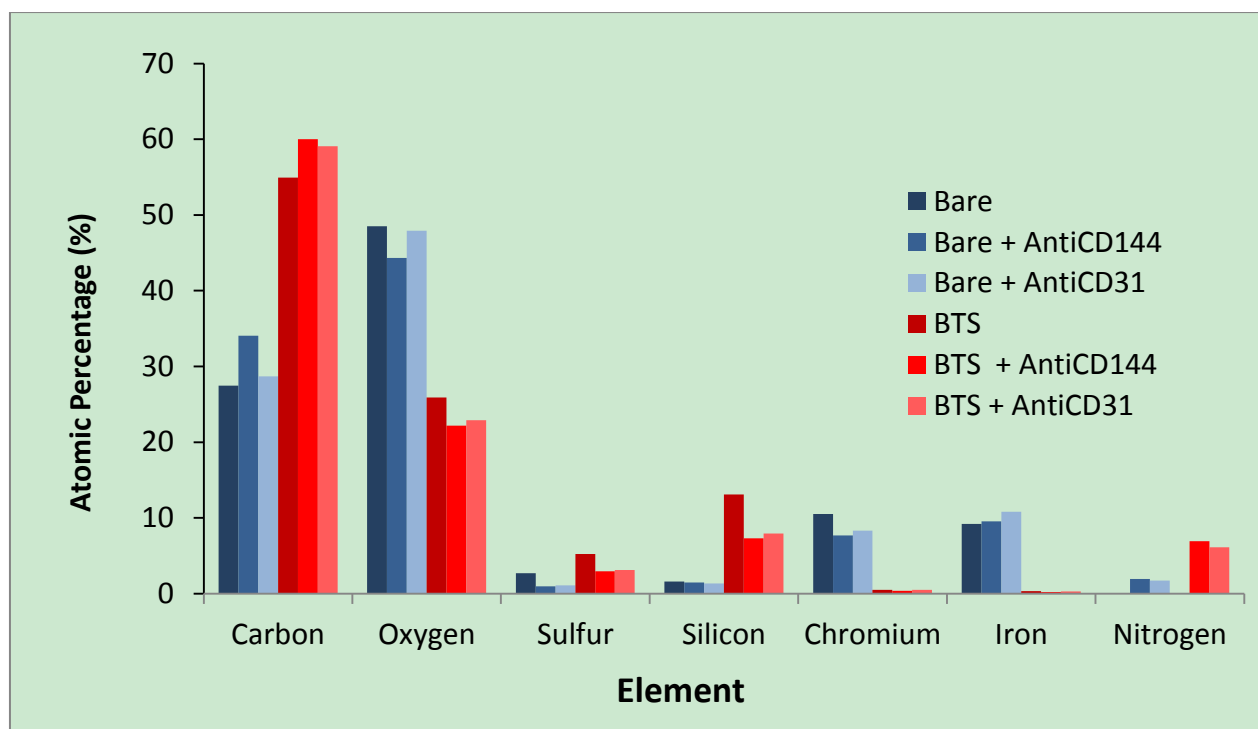


Figure 2 XPS elemental analysis of bare samples with and without antibodies (blue), and BTS coated samples with and without antibodies (red).

3.2 Surface Coverage of HUVECs on Functionalized Stainless Steel

Anti-human CD144 (VE-cadherin) was attached to the metal surface in order to facilitate binding to the VE-cadherin surface receptors on endothelial cells. The following conditions were assessed in this experiment: i) bare steel, ii) bare steel that had been incubated in a solution of antibodies (bare + antibody), iii) BTS alone (no antibodies on the surface) and iv) BTS + antibody, with 3 samples being tested for each condition.

In terms of re-endothelialization, the graph in Figure 3 compares the coverage of HUVECs between conditions as well as cell morphology. Cells were fixed and imaged following 3 days of growth on the surfaces. Each of the percentages shown has been normalized relative to the control, 'bare' sample. Fluorescence images representing each of the conditions are shown in Figure 3 A-D. HUVECs adhering to the bare surface had reduced expression of VE-cadherin and did not properly differentiate and failed to cover the whole surface. In this condition a large number of dead cells were found in the medium, and the cells remaining on bare surface had abnormal morphology as marked by arrows. CD144 molecule distribution appeared to be lacking in the majority of cells. Importantly HUVECs adhered one to another (clumps) and did not form a confluent monolayer.

When anti-CD144 was coated on the bare surface, HUVECs were captured on the surface, however significant numbers of clumps were observed on the surface, suggesting impairment of cell adhesion. In both Figure 3A and 3B, the large masses of cells suggest that these conditions are not suitable for cell growth. In Figure 3C, HUVECs poorly adhered to BTS linker coated surfaces and there was overall sparse coverage of cells, with reduced expression of CD144. In this treatment condition, clumps of HUVECs also appear to be present, indicating the presence of agglomerated

cells. BTS + anti-CD144 antibody condition showed a statistically significantly higher number of cells adhering and more even coverage on modified steel surface, compared to the bare control with an approximately 13% increase in number of cells observed ($p < 0.05$). Only this condition showed normal morphology of HUVECs undergoing differentiation and the cell layer was fully confluent (Figure 3D).

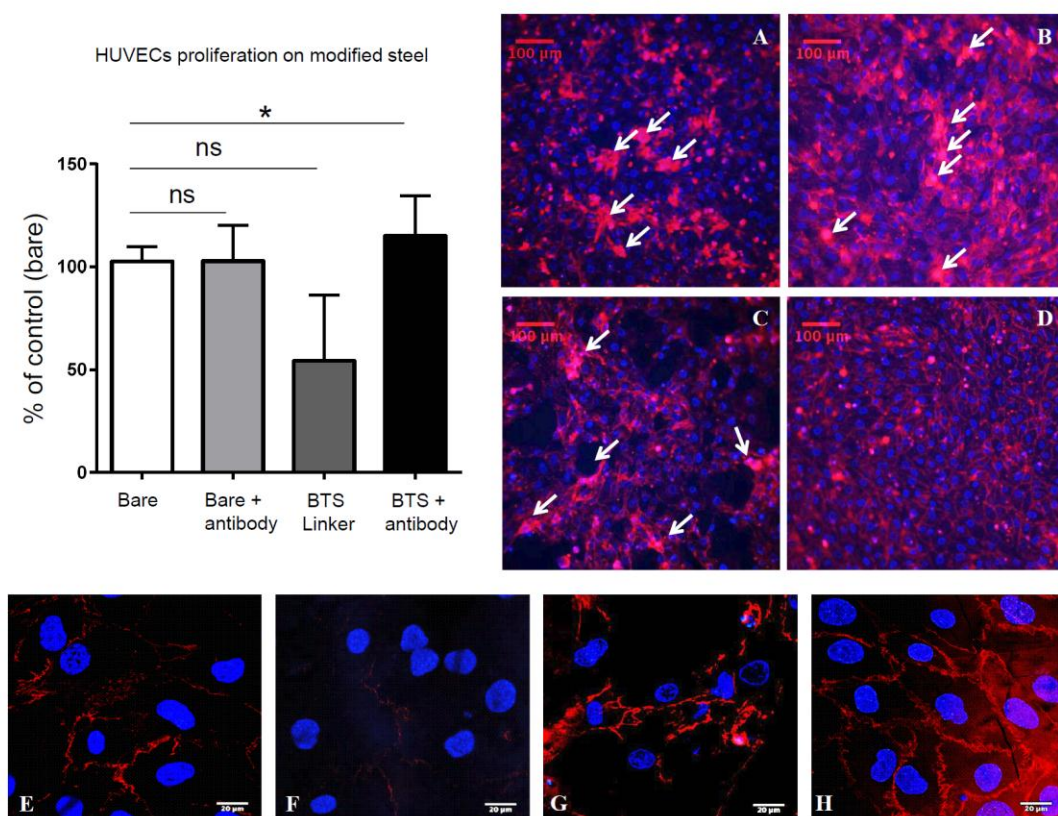


Figure 3 HUVEC proliferation on different treated surfaces. Blue represents DAPI nuclear stain and red represents Alexa Fluor® 594 anti-human CD144. (A) Bare steel, (B) Bare + antibody, (C) BTS only, (D) BTS + antibody. Each image was obtained at 10x magnification. Higher magnification of confocal image were obtained for (E) Bare steel, (F) Bare + antibody, (G) BTS only, (H) BTS + antibody. (*) represents $p < 0.05$. Error bars represent the standard deviation of the mean, (N = 3).

The BTS + antibody surface treatment yielded highly organized spatial localization of CD144 and normal morphology, as evidenced by the defined cell-cell adherens junctions between cells. Confocal microscopy images of HUVECs are shown in Figure 3 E-H. They were obtained at 40x magnification, and clearly show the presence of cell-cell adherens junctions between HUVECs, which are enhanced in the BTS + antibody group. These images provide a closer look at the cell morphology. As illustrated in Figure 3 E-H, the expression of VE-cadherin is re-localized in conditions 'bare', 'bare + antibody' and abnormally distributed on cell surfaces. Interestingly VE-cadherin staining sharply defined confluent cells as a monolayer in the BTS + antibody condition. Image analysis found 70% less visible VE-cadherin on bare steel surfaces compared to BTS + antibody surfaces.

3.3 Surface Coverage of HAoECs on Functionalized Stainless Steel

To further test the re-endothelization method on a modified steel surface, an immortalized human aortic endothelial cell line was used, together with a different capture antibody. In contrast to our HUVEC experiments, anti-human CD31 (platelet endothelial cell adhesion molecule, PECAM-1) was adsorbed on the steel surface so that aortic cells expressing PECAM-1 could be captured. The same four conditions as previously noted (bare steel, bare + antibody, BTS and BTS + antibody) were maintained, and cells were allowed to grow for 3 days before staining and fixing. In Figure 4, steel surface coverage by aortic endothelial cells is compared between the treatment conditions, and each value has been normalized to the 'bare' control.

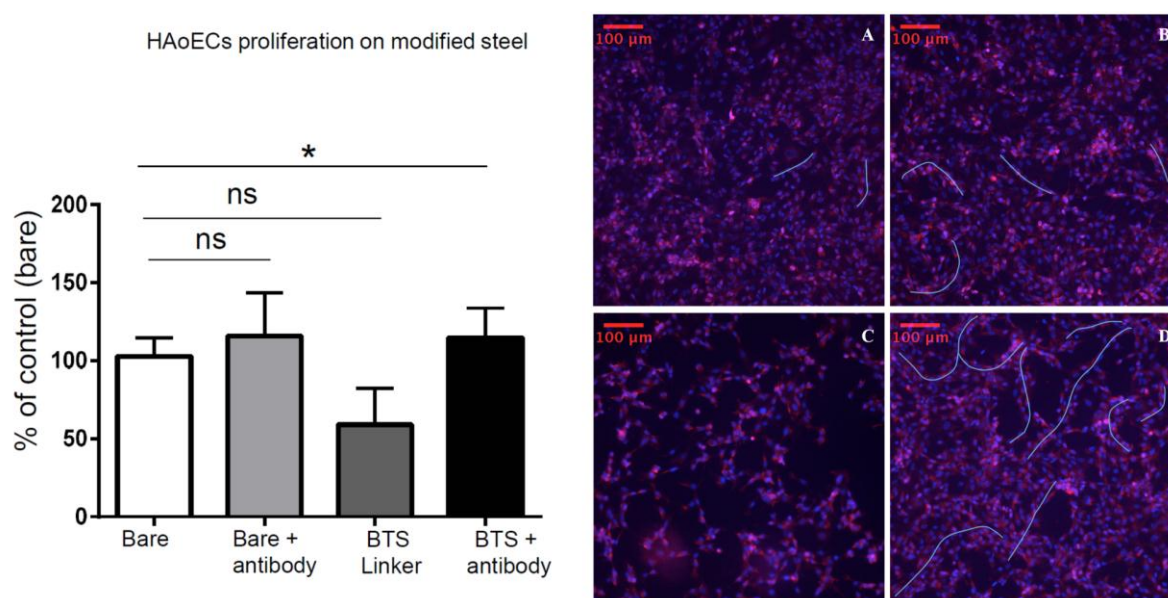


Figure 4 HAoEC proliferation on different treated surfaces. Blue represents DAPI nuclear stain and red represents Alexa Fluor® 594 anti-human CD144. (A) Bare steel, (B) Bare + antibody, (C) BTS only, (D) BTS + antibody. Each image was obtained at 10x magnification. (*) represents $p < 0.05$. Error bars represent the standard deviation of the mean, (N = 5).

Both 'bare' and 'bare + antibody' conditions (Figure 4A and 4B) show good surface coverage of HAoECs but overall cell morphology was significantly lost in these conditions. Unfortunately the cells grown in these conditions were mostly random, with no polarity visible. Furthermore HAoECs plated on BTS linker did not grow to confluency and surface coverage and cell differentiation/polarization was significantly reduced (Figure 4C). In this case, the overall cell coverage was very sparse, and a significant amount of steel was exposed.

However in Figure 4D (BTS + antibody), the cells appear polarized in many sections. This is indicated by the thin curves showing directional migration and polarization. The HAoECs are also expressing VE-cadherin, and are growing close to one another, thereby masking large areas of exposed steel. However there still appears to be a few empty spaces of exposed steel present. The BTS + antibody condition showed significant difference in the percentage of cells captured, compared to the bare control of approximately 12% ($p < 0.05$). Once again we analyze the morphology of the aortic cells to ensure that the linker + antibody condition yielded healthier cells.

4. Discussion

Prior work by Lee *et al.* [26] has demonstrated that steel stents simply adsorption-coated with anti-VE-cadherin were re-endothelialized faster *in vivo* than stents coated with anti-CD34. (VE-cadherin is a key adhesion molecule on the surface of endothelial cells that is a component of endothelial cell-to-cell adherens junctions, and also plays a key role in the maintenance of vascular integrity [31, 32]). In this work, we show that BTS-modified medical grade steel offers the possibility to attach both intact antibodies and Fab' fragments to the substrate surface in a highly robust fashion as discussed previously [30]. This system displays enhanced stability and continued capability to bind antigenic species even following harsh rinsing conditions. The latter behavior is undoubtedly associated with the formation of the highly stable S-S bond for both whole antibody and fragment cases.

Here we confirm that the surface modified with BTS linker + antibody displays an enhanced capacity to re-endothelialize and mask the exposed steel surface, relative to the currently available bare metal stents. Not only did the number of cells that adhered on and covered the BTS linker + antibody condition reach a statistically significant level, but these cells displayed a normal pattern of differentiation and further, they achieved confluency. This suggests that adherent junction formation is favoured in this condition. The cells are elongated and there are far fewer clumps present in this state, indicating that this treatment may be favourable for HUVEC growth. We believe that this layer of cells should be stable on the surface as a result of correctly formed adherent junctions and proper elongation.

In contrast, cells seeded on other surfaces have agglomerated into large masses. Upon adhesion onto a surface it is important for endothelial cells to be able to migrate and proliferate. Migration of cells is very important when it comes to surface coverage wound healing [33]. This is necessary for the formation of a healthy endothelium. When cells are unable to migrate sufficiently it results in formation of an unhealthy monolayer, and can lead to poor viability of cells. On poorly adherent surfaces this inhibits HUVEC tethering and adhesion, and as a result these cells will die. Since others treatments showed HUVECs clumping one to another that suggests reduced adhesion, migration, and differentiation capacities in these conditions. HUVECs grow on adherent surfaces by dividing and migrating towards unoccupied areas. The cells stop growing when they come into close contact.

With the single exception of the BTS linker + antibody condition, HUVECs grown on other surfaces will likely undergo apoptosis due to the fact that they lose adhesion molecules and migration capacity. Interestingly, in the BTS linker + antibody condition they form a healthy endothelium on the material surface, and are thus clearly expected to be biocompatible when implanted on a genuine steel-based stent. Thus, it is clear that both the morphology and surface coverage of HUVECs are favoured on the BTS + antibody condition. Given this result, application of another physiologically relevant cell line, human aortic endothelial cells, was explored in terms of analogous capture experiments.

Consistently, aortic cells proliferating on 'bare', 'bare+antibody', and 'BTS linker' appeared to be less confluent and were separated by large spaces of exposed steel. This is obviously not optimal for the formation of a healthy endothelium. Exposure of the metal surface also has the potential to elicit a thrombotic response *in vivo*. While agglomeration of aortic cells is minimal, the cells growing on these surfaces are not polarized. Given that the aorta is shaped like an arch,

aortic cells that migrate in this pattern *in vitro* are likely to retain the biological functions that they would have *in vivo*. It has been suggested that cadherins play a role in the polarization of endothelial cells [34]. Despite the fact that a greater number of cells were captured by the bare + antibody condition, fluorescence microscopy determined that formation of a healthier endothelium was favoured on the BTS + antibody condition.

5. Conclusions

We have successfully applied our biologically active surface coating towards the capture of two endothelial cell lines. *In vitro* cell cultures for HUVECs revealed that their morphology and surface coverage with a statistically significant increase in number of cells was favoured when they were grown on the BTS + antibody condition, compared to other treatments (bare, bare + antibody, BTS). The adherence and junctions between cells of this cell line and primary cells were not hindered. Overall, these cells appeared to form a healthy endothelium on the steel substrate. With regard to HAoECs, the morphology of these cells were optimal on the BTS + antibody condition, much like the HUVECs. These cells displayed characteristics such as polarization, which is a commonly observed phenomenon when aortic cells proliferate in their native environment. Our proposed surface coating has the potential to resist stent thrombosis and restenosis, provided that adherent cells are able to completely cover the surface and prevent exposure of the bare steel.

Acknowledgments

We thank Dr. Peter Brodersen from Surface Interface Ontario for XPS analysis, and Miria Bartolini and Judith Cathcart from the Advanced Optical Microscopy Facility at the MaRS Center Toronto for fluorescence analysis. We also thank Paul Turgeon and Dr. Philip Marsden from St. Michael's Hospital, Toronto for providing HUVECs, and Professors Heyu Ni and Alex Romaschin of the Keenan Research Centre, St. Michael's Hospital for use of lab facilities and many helpful comments. This work was supported by Canadian Institutes of Health Research (MOP 68986 and MOP 119551) and the Natural Sciences and Engineering Research Council of Canada (to MT). Equipment was supported by funds from the Canada Foundation for Innovation, St. Michael's Hospital, and Canadian Blood Services. I. Yougbaré is a recipient of a Canadian Blood Services postdoctoral fellowship.

Author Contributions

RR performed the experiments, completed data analysis, and wrote the manuscript. BD contributed data analysis, wrote portions of the manuscript, and edited the manuscript. IY and JF contributed experimental design and expertise to this work. MT oversaw the work, contributed experimental design, wrote portions of the manuscript, and edited the manuscript.

Competing Interests

All authors declare no competing financial interest.

References

1. GBD 2013 Mortality and Causes of Death Collaborators, Global, regional, and national age-sex specific all-cause and cause-specific mortality for 240 causes of death, 1990-2013: a systematic analysis for the Global Burden of Disease Study 2013. *Lancet*. 2015; 385: 117-171.
2. Nazneen F, Herzog G, Arrigan DW, Caplice N, Benvenuto P, Gavin P. Surface chemical and physical modification in stent technology for the treatment of coronary artery disease. *J Biomed Mater Res B Appl Biomater*. 2012; 100: 1989-2014.
3. Avci-Adali M, Perle N, Ziemer G, Wendel HP. Current concepts and new developments for autologous in vivo endothelialisation of biomaterials for intravascular applications. *Eur Cell Mater*. 2011; 21: 157-176.
4. Mehta D, George SJ, Jeremy JY, Izzat MB, Southgate KM, Bryan AJ, et al. External stenting reduces long-term medial and neointimal thickening and platelet derived growth factor expression in a pig model of arteriovenous bypass grafting. *Nat Med*. 1998; 4: 235-239.
5. Sumpio BE, Riley JT, Dardik A. Cells in focus: Endothelial cell. *Int J Biochem Cell Biol*. 2002; 34: 1508-1512.
6. Lusis AJ. Atherosclerosis. *Nature*. 2000; 407: 233-241.
7. Davies SW. Clinical presentation and diagnosis of coronary artery disease: Stable angina. *Br Med Bull*. 2001; 59: 17-27.
8. Heidenreich PA, Trogon JG, Khavjou OA, Butler J, Dracup K, Ezekowitz MD, et al. Forecasting the future of cardiovascular disease in the United States: A policy statement from the American Heart Association. *Circulation*. 2011; 123: 933-944.
9. Jeewandara TM, Wise SG, Ng MKC. Biocompatibility of coronary stents. *Materials*. 2014; 7: 769-786.
10. Ravindranath R, Romaschin A, Thompson M. In vitro and in vivo cell-capture strategies using cardiac stent technology - a review. *Clin Biochem*. 2016; 49: 186-191.
11. Joner M, Finn AV, Farb A, Mont EK, Kolodgie FD, Ladich E, et al. Pathology of drug-eluting stents in humans: Delayed healing and late thrombotic risk. *J Am Coll Cardiol*. 2006; 48: 193-202.
12. Sousa JE, Costa MA, Abizaid AC, Rensing BJ, Abizaid AS, Tanajura LF, et al. Sustained suppression of neointimal proliferation by sirolimus- eluting stents. *Circulation*. 2001; 104: 2007-2011.
13. Grove ECL, Kristensen SD. Stent thrombosis: Definitions, mechanisms and prevention. *Eur Soc Cardiol J Cardiol Pract*. 2007; 5: 1-5.
14. Kushwaha M, Anderson JM, Bosworth CA, Andukuri A, Minor WP, Lancaster JR, et al. A nitric oxide releasing, self- assembled peptide amphiphile matrix that mimics native endothelium for coating implantable cardiovascular devices. *Biomaterials*. 2010; 31: 1502-1508.
15. Andukuri A, Kushwaha M, Tambralli A, Anderson JM, Dean DR, Berry JL, et al. A hybrid biomimetic nanomatrix composed of electrospun polycaprolactone and bioactive peptide amphiphiles for cardiovascular implants. *Acta Biomater*. 2011; 7: 225-233.
16. Karagkiozaki VC, Logothetidis SD, Kassavetis SN, Giannoglou GD. Nanomedicine for the reduction of the thrombogenicity of stent coatings. *Int J Nanomedicine*. 2010; 5: 239-248.

17. Thompson M, Sheikh S, Blaszykowski C, de los Santos Pereira A, Rodriguez-Emmenegger C. Biological-fluid surface interactions in detection and medical devices. Cambridge: Royal Society of Chemistry Publishing; 2016.
18. Whelan DM, van der Giessen WJ, Krabbendam SC, van Vliet EA, Verdouw PD, Serruys PW, et al. Biocompatibility of phosphorylcholine coated stents in normal porcine coronary arteries. *Heart*. 2000; 83: 338-345.
19. Thierry B, Winnik FM, Merhi Y, Silver J, Tabrizian M. Bioactive coatings of endovascular stents based on polyelectrolyte multilayers. *Biomacromolecules*. 2003; 4: 1564-1571.
20. Kipshidze N, Dangas G, Tsapenko M, Moses J, Leon MB, Kutryk M. Role of the endothelium in modulating neointimal formation: Vasculoprotective approaches to attenuate restenosis after percutaneous coronary interventions. *J Am Coll Cardiol*. 2004; 44: 733-739.
21. Urbich C, Dimmeler S. Endothelial progenitor cells: Characterization and role in vascular biology. *Circ Res*. 2004; 95: 343-353.
22. Losordo DW, Isner JM, Diaz-Sandoval LJ. Endothelial recovery: The next target in restenosis prevention. *Circulation*. 2003; 107: 2635-2637.
23. Werner N, Junk S, Laufs U, Link A, Walenta K, Bohm M, et al. Intravenous transfusion of endothelial progenitor cells reduces neointima formation after vascular injury. *Circ Res*. 2003; 93: e17-e24.
24. Kong D, Melo LG, Mangi AA, Zhang L, Lopez-Illasaca M, Perrella MA, et al. Enhanced inhibition of neointimal hyperplasia by genetically engineered endothelial progenitor cells. *Circulation*. 2004; 109: 1769-1775.
25. Chang HK, Kim P-H, Kim DW, Cho H-M, Jeong MJ, Kim DH, et al. Coronary stents with inducible VEGF/HGF-secreting UCB-MSCs reduced restenosis and increased re-endothelialization in a swine model. *Exp Mol Med*. 2018; 50: 114.
26. Lee JM, Choe W, Kim BK, Seo WW, Lim WH, Kang CK, et al. Comparison of endothelialization and neointimal formation with stents coated with antibodies against CD34 and vascular endothelial-cadherin. *Biomaterials*. 2012; 33: 8917-8927.
27. Li J, Li D, Gong F, Jiang S, Yu H, An Y. Anti-CD133 Antibody immobilized on the surface of stents enhances endothelialization. *J Biomed Res Int*. 2014; 2014: 1-9.
28. Larsen K, Cheng C, Tempel D, Parker S, Yazdani S, den Dekker WK, et al. Capture of circulatory endothelial progenitor cells and accelerated re-endothelialization of a bio-engineered stent in human ex vivo shunt and rabbit denudation mode. *Eur Heart J*. 2012; 33: 120-128.
29. Choi WG, Kim SH, Yoon HS, Lee EJ, Kim DW. Impact of an endothelial progenitor cell capturing stent on coronary microvascular function: Comparison with drug-eluting stents. *Korean J Intern Med*. 2015; 30: 42-48.
30. Benvenuto P, Neves MA, Blaszykowski C, Romaschin A, Chung T, Kim S-R, et al. Adlayer-mediated antibody immobilization to stainless steel for potential application to endothelial progenitor cell capture. *Langmuir*. 2015; 31: 5423-5431.
31. Meng W, Takeichi M. Adherens junction: Molecular architecture and regulation. *Cold Spring Harb Perspect Biol*. 2009; 1: 1-13.
32. Vestweber D. VE-Cadherin: The major endothelial adhesion molecule controlling cellular junctions and blood vessel formation, *Arterioscler Thromb Vasc Biol*. 2008; 28: 223-232.
33. Franz CM, Jones GE, Ridley AJ. Cell migration in development and disease. *Dev Cell*. 2002; 2: 153-158.

34. Halbleib JM, Nelson WJ. Cadherins in development: Cell adhesion, sorting, and tissue morphogenesis. *Genes Dev.* 2006; 20: 3199-3214.



Enjoy *Recent Progress in Materials* by:

1. [Submitting a manuscript](#)
2. [Joining in volunteer reviewer bank](#)
3. [Joining Editorial Board](#)
4. [Guest editing a special issue](#)

For more details, please visit:

<http://www.lidsen.com/journals/rpm>